Electronic Structure Basis for the Extraordinary Magnetoresistance in WTe_{2}

I. Pletikosić, Mazhar N. Ali, A. V. Fedorov, R. J. Cava, and T. Valla

Phys. Rev. Lett. **113**, 216601 — Published 19 November 2014

DOI: 10.1103/PhysRevLett.113.216601

Electronic structure basis for the extraordinary magnetoresistance in WTe_2

I. Pletikosić,[1,2] Mazhar N. Ali,[3] A. V. Fedorov,[4] R. J. Cava,[3] and T. Valla[2]

[1] *Department of Physics, Princeton University, Princeton, New Jersey 08544, USA*
[2] *Condensed Matter Physics and Materials Science Department, Brookhaven National Laboratory, Upton, New York 11973, USA**
[3] *Department of Chemistry, Princeton University, Princeton, New Jersey 08544, USA*
[4] *Advanced Light Source, Lawrence Berkeley National Laboratory, Berkeley, California 94720, USA*

The electronic structure basis of the extremely large magnetoresistance in layered non-magnetic tungsten ditelluride has been investigated by angle-resolved photoelectron spectroscopy. Hole and electron pockets of approximately the same size were found at low temperatures, suggesting that carrier compensation should be considered the primary source of the effect. The material exhibits a highly anisotropic Fermi surface from which the pronounced anisotropy of the magnetoresistance follows. A change in the Fermi surface with temperature was found and a high-density-of-states band that may take over conduction at higher temperatures and cause the observed turn-on behavior of the magnetoresistance in WTe_2 was identified.

PACS numbers: 72.15.Gd, 71.20.Be, 79.60.Bm

An extremely large positive magnetoresistance was recently discovered in several non-magnetic materials including Cd_3As_2, WTe_2, and $NbSb_2$ [1–3]. At low-temperatures, for each of these a several orders of magnitude increase in resistivity was found with no evidence of saturation in very high fields, differentiating them greatly from simple metals where the magnetoresistance is usually small, quadratic only in low fields, and tends to saturate in high fields [4]. The understanding of the enormous magnetoresistance in these materials should start with the cognition of their electronic structure. In one of them, Cd_3As_2, the observed effect has been related to the three-dimensional (3D) Dirac nature of its electronic structure, where breaking of time-reversal symmetry in magnetic field removes the backscattering protection, leading to a large increase of resistivity. For the other two materials, however, the calculated Fermi surfaces and the overall electronic band-structure do not show resemblance to a 3D Dirac semimetal [2, 3]. As a matter of fact, both materials have complicated band-structure with multiple, two-carrier Fermi pockets and display a very anisotropic magnetoresistance, rapidly disappearing with increasing temperature, suggesting that the fine details of the electronic structure play a significant role.

Our study focuses on WTe_2, a layered transition metal dichalcogenide in which each tungsten (transition metal) layer is surrounded by two tellurium (chalcogen) layers. Owing to pronounced bonding between W atoms (bond length is only about 4% larger than in tungsten metal), the layers are structurally distorted from the usual hexagonal network: tungsten atoms form slightly buckled, well separated zig-zag chains, and the tellurium octahedra surrounding each W atom distort to accommodate them [2, 5]. The layers are held together by van der Waals interaction, and are sequentially rotated by 180° to account for the layer buckling.

The temperature dependence of resistivity, Hall coefficient and thermoelectric power have been successfully explained for WTe_2 by a three-carrier model [6]. The three bands, however, have not been clearly identified due to the complex band structure of WTe_2, nicely exemplified in a density functional band structure calculation by Augustin *et al.* [5]. The experimental, angle-resolved photoemission spectroscopy (ARPES) results from the same study were not of sufficiently high angular and energy resolution to get any conclusive insight into the bands in the vicinity of the Fermi level.

Here, we investigate the low energy electronic structure of WTe_2 using high-resolution ARPES. We find that the configuration and the temperature dependence of its Fermi surface, as well as the details of the band dispersion along the direction of the metallic chains explain the main features of the enormous magnetoresistive effect.

Single crystal platelets of WTe_2 were grown via bromine vapor transport method described in [2]. The samples were glued to the holder by a conductive epoxy resin and cleaved in ultrahigh vacuum ($p < 10^{-8}$ Pa) just before the measurements. Sample cooling was provided through contact with cryostats filled with liquid helium or liquid nitrogen. The ARPES measurements were conducted at the National Synchrotron Light Source at BNL ($h\nu = 21\,\mathrm{eV}$), and at the Advanced Light Source at LBNL (38–78 eV) using Scienta analyzers with total experimental resolution of ~15 meV and <0.2°. The two-dimensional Brillouin zone mapping was accomplished by sample rotation perpendicularly to the analyzer slit, in steps of 2°, 0.5°, or 0.25°.

Structural reduction to well-separated WTe_2 layers, and within each layer to chains of tellurium-surrounded tungsten atoms leaves a substantial mark in the low-energy band structure. The constant energy maps at the Fermi level and 100 meV below, shown in Fig. 1, exhibit pronounced unidirectionality, in the sense that the charge carriers acquire only a small momentum perpendicular

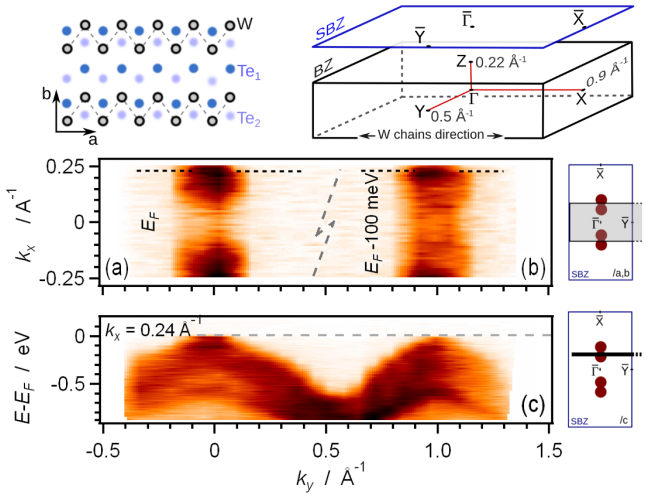

Figure 1. Electronic structure of WTe_2 mapped by ARPES at 20 K through two extended surface Brillouin zones along the $\bar{\Gamma}-\bar{Y}$ (k_y) direction. Constant energy maps were extracted (a) at the Fermi level, E_F, and 100 meV below (b). Only a portion of the zone that extends to $\pm 0.9\,\text{Å}^{-1}$ was mapped along the $\bar{\Gamma}-\bar{X}$ (k_x) direction. (c) Band dispersion along $\bar{\Gamma}-\bar{Y}$ at the point $k_x = 0.24\,\text{Å}^{-1}$ with the highest intensity at the Fermi level. Excitation energy $h\nu = 21\,\text{eV}$; sampling around $k_z = 2.7\,\text{Å}^{-1}$ (Γ_6). Top: Schematic view of the crystal structure, and bulk (BZ) and surface (SBZ) Brillouin zones. Right: a sketch of the ARPES scans performed in (a)–(c).

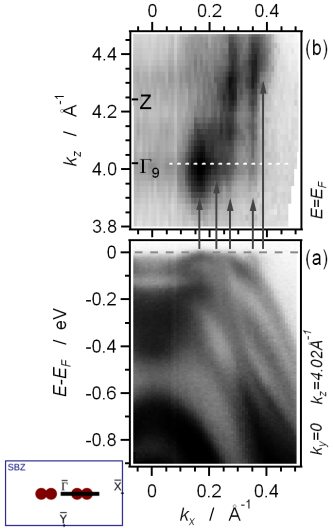

Figure 2. (a) Dispersion of WTe_2 bands along the $\bar{\Gamma}-\bar{X}$ direction taken with the excitation energy of $h\nu = 54\,\text{eV}$. The k_z dependence of the states at the Fermi level, E_F, shown in (b), was obtained by combining many of such spectra taken in the 40–70 eV range of excitation energies. The band structure in (a) represents the cut at $k_z = 4.02\,\text{Å}^{-1}$, which is the center of the ninth extended Brillouin zone, Γ_9.

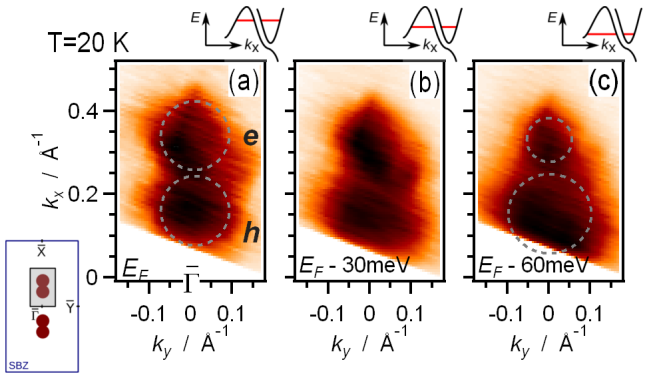

Figure 3. (a)–(c) Constant energy contours at T=20 K in the region of the Brillouin zone where the bands of WTe_2 cross the Fermi level, E_F. Electron-like and hole-like pockets are marked with e and h, respectively. Excitation energy was $h\nu = 21\,\text{eV}$. The mapping has been carried out by 0.5° polar rotation. Dashed circles have been added as a guide to the eye. Above: a sketch of the band structure and constant energy cuts being made in (a)–(c).

to the chains (k_y of about $0.07\,\text{Å}^{-1}$), and several times larger along the chains. The carrier scattering pattern, which is, to the first approximation, an autocorrelation map of the Fermi surface, will inherit this directionality, meaning that the charge carriers will preferably scatter along the chains, regardless of the current direction.

Figure 1(c) shows that the band dispersion in the perpendicular direction (along the b-axis) is modest, amounting to some 0.6 eV over the whole Brillouin zone. Even though Fig. 1(a) shows only a part of the Brillouin zone, which extends to $\pm 0.90\,\text{Å}^{-1}$ in the chain direction (due to limited angular window of the ARPES scan), further scanning found no bands close to the Fermi level except those along $\bar{\Gamma}-\bar{X}$. One such scan is shown in Fig. 2(a). The only states crossing the Fermi level are found for k_x between $0.15\,\text{Å}^{-1}$ and $0.40\,\text{Å}^{-1}$, in agreement with density functional predictions in Refs. 5 and 2.

The photon-energy dependency measurements of a band dispersion can be translated into its k_z dependence by $\hbar k_z = [2m_e(E_{\text{kin}}\cos^2\vartheta - V_o)]^{1/2}$. The value of the free-electron final state band minimum V_o of $-11.5\,\text{eV}$, adopted from Ref. 5, adequately reproduced the band structure periodicity over a few Brillouin zones. As the Brillouin zone size in the $\Gamma-Z$ (k_z) direction perpendicular to WTe_2 layers is only $0.446\,\text{Å}^{-1}$, the photoemission probes the higher order zones (in the extended scheme) even with the lowest excitation energies. In our case this was the sixth zone for 21 eV photons, and the ninth and tenth zone for the 40–70 eV range.

The band dispersion spectrum along the k_x (chain direction) at $k_y = 0$ in Fig. 2(a) has been chosen from the hv dependence map as it shows most features at the Fermi level. Two bands found at k_x of $0.28\,\text{Å}^{-1}$ and $0.36\,\text{Å}^{-1}$, are strikingly flat along k_z, exhibiting localization within the WTe_2 layers. The intensity arising from the band centered around $k_x = 0.16\,\text{Å}^{-1}$ has only a limited k_z extent around Γ and reaches to about one half

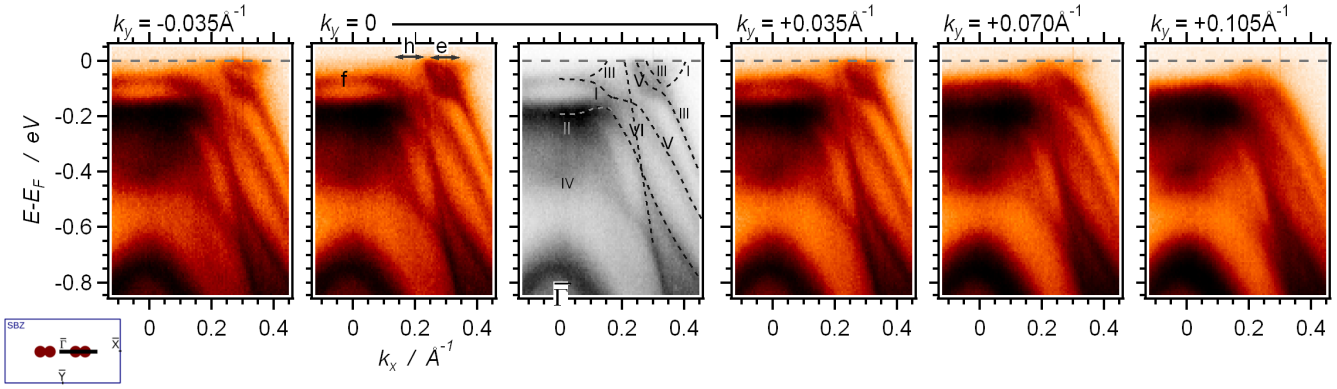

Figure 4. High resolution band dispersion ARPES scans along a few lines parallel to the $\bar{\Gamma}-\bar{X}$ direction of the surface Brillouin zone. Evolution of a tiny electron pocket is visible around $k_x = 0.33\,\text{Å}^{-1}$, as well as two hole-like bands traversing the Fermi level around $k_x = 0.22\,\text{Å}^{-1}$. The spectra have been extracted from a map taken with a 0.5° step in the polar angle. Excitation energy was $h\nu = 68\,\text{eV}$. The $k_y = 0$ spectrum is shown twice for the purpose of tracing and labeling the bands, following their overall shape and ordering from Figs. 6 and 7 in Ref. 5.

of the bulk Brillouin zone. As localized states often exhibit large ARPES intensity variations with the photon energy used, it is not clear if this represents the actual k_z range of the state or if it is an effect of varying optical transition-probabilities in photoemission: the same band reappears at much lower intensity around $k_z = 4.47\,\text{Å}^{-1}$ (Γ_{10}), and two others can be identified, following the arrows in Fig. 2, with notable variation in intensity. Bands with such a low dispersion along the c-axis result in open orbits of charge carriers under the magnetic field, which manifests itself in the pronounced anisotropy of the magnetoresistance reported in [2].

As all the bands crossing the Fermi level are also visible with 21 eV photon energy we were able to map them in higher resolution. The ARPES intensity maps shown in Fig. 3 represent constant energy contours of the states at and slightly below the Fermi level. The states appear as two distinct pockets. The pocket at $0.33\,\text{Å}^{-1}$ decreases in size as we go lower in energy, indicating that it is the very bottom of a band. The opposite happens with the pocket around $0.16\,\text{Å}^{-1}$, and its area doubles going from the Fermi level to just 60 meV below. The former thus represents an electron-like (e) pocket, and the latter a hole-like (h) one. The size of the pockets at the Fermi level is almost exactly the same, $0.018\,\text{Å}^{-2}$. Taking into account spin degeneracy and the fact that there are two such pockets in the surface Brillouin zone, it follows that the carrier concentration in the electron pockets is about $1.8 \cdot 10^{13}\,\text{cm}^{-2}$ and is nearly perfectly compensated by the same concentration of holes. This is reminiscent of the compensation in Mg, Zn, and Bi, all of which exhibit large magnetoresistance, although with saturation at high field [4, 7–11]. When the Fermi surfaces for both electrons and holes are closed, i.e. not connected across the borders of the Brillouin zone, the compensation leads to a quadratic rise of magnetoresistance in high magnetic fields (see pp. 104–106 in [4]). And indeed, a quadratic rise was found for WTe_2 in Ref. 2 for the fields above 1 T, and all up to 60 T. This well balanced compensation is likely the cause of the high saturation value of magnetoresistance: it is reached in the magnetic fields that scale as the reciprocal of the difference of charge densities, while its magnitude scales as the square of that value (see pp. 28–31 in [4]). Thus, the better the compensation, the higher the magnetoresistance limit. Unlike any other known system at this time, the magnetoresistance in WTe_2 does not appear to saturate even at the field of 60 T (in Bi, for example, it saturates by 40 T [11]). The extreme similarity of the pockets and the lack of deviation from a quadratic dependence of the magnetoresistance to very high fields implies that WTe_2 may be the first example of a perfectly compensated semimetal [2]. It is important to note that the closeness of the two pockets as well as their overall smallness may play an important role in the magnetoresistance: the former through an increased scattering between the neighboring orbits and the latter through the relation of the time needed to complete an orbit to the mean scattering time.

A sequence of high resolution ARPES spectra taken along the chain direction, Fig. 4, details the evolution of the electron pocket (e) as k_y is swept across $\bar{\Gamma}$: the whole pocket is accommodated within $\pm 0.075\,\text{Å}^1$ in both directions, reaches down to 80 meV below the Fermi level, and approaches the elbow of the rightmost band to within ~20 meV. Exploiting the similarities in the shape and ordering of the measured bands to the calculated band structure, the bands along $\bar{\Gamma}$-$\bar{X}$ in Fig. 4 have been labeled as in Ref. 5. The electron pocket is likely formed by an avoided hybridization of a tungsten $5d$ band (I) and a tellurium $5p$ band (III). This band, while returning from above the Fermi level, and the band originating from tungsten orbitals (V), make the hole pocket [5]. To

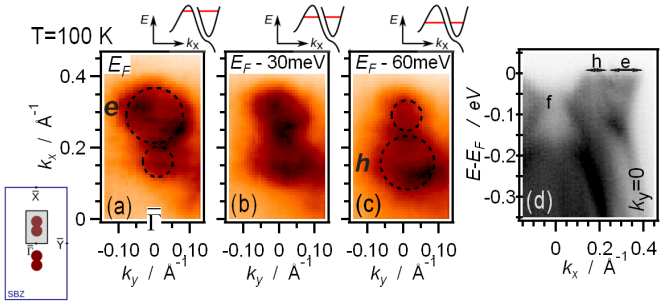

Figure 5. (a)–(c) Constant energy contours of the electron (e) and hole (h) pockets in WTe_2 band structure close to the Fermi level, E_F, taken at T=100 K. The mapping has been carried out by polar rotations of 0.25°. (d) Low energy band dispersion acquired along the $\bar{\Gamma} - \bar{X}$ direction at T=100 K.

add to the complexity of the band structure, a linear band (VI) dispersing at $v = 5$ eVÅ passes right through the hole pocket; its impact on the transport in WTe_2 is currently unknown, but probably just adds a constant contribution independent of the temperature.

Although the general shape of the density functional theory derived bands in Refs. 5 and 2 corresponds to what has been measured here, quantitative agreement is far from satisfying. As an example: the separation between the elbow shaped band (III→V) and the electron pocket (I→III) appears exaggerated in the calculations both in momentum and energy; the fast dispersing band (VI) that is crossing the Fermi level at 0.2 Å^{-1} is present in [5] but is missing or appears highly hybridized in [2]; most calculated bands turn out to be dilated in momentum, and for some, considerable shifts in energy can be noted. This calls for a better theoretical modeling of the system.

The relative increase of magnetoresistance with the magnetic field in WTe_2 weakens with increasing temperature. Our data show a dramatic change of the Fermi surface as the temperature is raised from 20 K to 100 K. A constant energy map taken at 100 K, Fig. 5(a), shows at the Fermi level a large electron pocket centered at $k_x = 0.30$ Å^{-1} and a tiny hole pocket around $k_x = 0.16$ Å^{-1}. The temperature increase caused the bands forming the pockets to become electron doped by about 30 meV, as the contour with largely compensated electrons and holes that represented the Fermi surface at 20 K is now found at a 30 meV lower energy. Such band shifts are common and arise from the thermal expansion of the crystal and coupling of the electrons to phonons. They tend to slow down and saturate, typically below a fraction of the Debye temperature [12, 13]. Assuming a continuous evolution as the temperature is turned down, a predominantly electron-like Fermi surface transforms into one with compensated electrons and holes. The upsurge of the magnetoresistance in WTe_2 as one approaches 0 K [2] suggests that the perfect balance is being reached in that limit.

While the increasing temperature spoils the compensation, reducing the magnetoresistive effect, a competing mechanism might be responsible for its complete diminishing [2] above 150 K. A band centered at $\bar{\Gamma}$, marked by f in Fig. 4, appears almost flat just about 65 meV below the Fermi level at 20 K, and does not change position when the temperature is raised to 100 K, Fig. 5(d). Its contour is also visible in the constant energy map at -100 meV (shown in Fig. 1(b)). While the band may be inert in transport at very low temperatures, Fermi-Dirac statistics works in favor of its conduction when the material is warmed: at 160 K, 1% of the electrons at this single energy level are thermally excited leaving conductive holes in the band, while this proportion at 80 K is only 0.01%. Combined with a high density of states related to its flatness, it is likely that at higher temperatures this band takes conduction over the bands that cross the Fermi level, and that the proximity of this band to the Fermi level is responsible for the *turn on* temperature behavior found in Ref. 2.

We have thus shown that tiny electron and hole pockets of equal size are the electronic basis for the unusual transport properties of WTe_2 at low temperatures. Extremely large magnetoresistance emerges from the resulting charge compensation, which has been shown to be temperature dependent, apparently approaching perfect compensation at very low temperatures. The pronounced anisotropy of the magnetoresistance is associated with higly anisotropic character of the Fermi surface and the proximity of the electron and hole pockets in momentum space along the direction of the metallic chains in this quasi one-dimensional material. A flat band lying below the Fermi level has been recognized as the source of the *turn on* temperature behavior of the magnetoresistance. Band dispersion measurements uncovered a complex structure in the vicinity of the Fermi level that calls for a more accurate band structure calculation and, based on it, a quantitative theoretical modeling of the magnetoresistance.

I.P. thanks Emil Tafra and Jun Xiong for enlightening discussions. This work was supported by the US Department of Energy, Office of Basic Energy Sciences, contracts No. DE-AC02-98CH10886 and DE-AC02-05CH11231, and ARO MURI program, grant W911NF-12-1-0461. ALS is operated by the US DOE under contract No. DE-AC03-76SF00098.

* ivop@princeton.edu

[1] T. Liang, Q. Gibson, M. N. Ali, M. Liu, R. J. Cava, and N. P. Ong, arXiv:1404.7794 (2014).

[2] M.N. Ali, J. Xiong, S. Flynn, J. Tao, Q.D. Gibson, L.M. Schoop, T. Liang, N. Haldolaarachchige, M. Hirschberger, N.P. Ong, and R.J. Cava, Nature 514, 205

(2014).
[3] K. Wang, D. Graf, and C. Petrovic, arXiv:1405.1719 (2014).
[4] A. B. Pippard, *Magnetoresistance in Metals* (Cambridge University Press, Cambridge, 1989).
[5] J. Augustin, V. Eyert, Th. Böker, W. Frentrup, H. Dwelk, C. Janovitz, and R. Manzke, Phys. Rev. B **62**, 10812 (2000).
[6] S. Kabashima, J. Phys. Soc. Jpn. **21**, 945 (1966).
[7] F. Y. Yang, K. Liu, K. Hong, D. H. Reich, P. C. Searson, and C. L. Chien, Science **284**, 1335 (1999).
[8] F. Yang, K. Liu, K. Hong, D. Reich, P. Searson, C. Chien, Y. Leprince-Wang, K. Yu-Zhang, and K. Han, Phys. Rev. B **61**, 6631 (2000).
[9] R. W. Stark, Phys. Rev. Lett. **9**, 482 (1962).
[10] L. Falicov, A. Pippard, and P. Sievert, Phys. Rev. **151**, 498 (1966).
[11] B. Fauqué, B. Vignolle, C. Proust, J.-P. Issi, and K. Behnia, New J. Phys. **11**, 113012 (2009).
[12] R. Paniago, R. Matzdorf, G. Meister, and A. Goldmann, Surf. Sci. **336**, 113 (1995).
[13] M. Cardona, Solid State Commun. 133, 3 (2005)